Molecular Dynamics Simulation of Atactic Polystyrene. 2. Comparison with Neutron Scattering Data

Hidemine Furuya,† M. Mondello,‡ Hyung-Jin Yang,§ and Ryong-Joon Roe*

Department of Materials Science and Engineering, University of Cincinnati, Cincinnati, Ohio 45221

R. W. Erwin and C. C. Han

National Institute of Standards and Technology, Gaithersburg, Maryland 20899

S. D. Smith

Procter and Gamble Company, Miami Valley Laboratories, Cincinnati, Ohio 45239

Received June 1, 1994®

ABSTRACT: Four polystyrene samples, some selectively deuterated, were synthesized by anionic polymerization for neutron scattering measurement. The four are a perdeuterated polystyrene, a polystyrene with its phenyl group deuterated, one with its aliphatic backbone deuterated, and a hydrogenous polystyrene. Neutron scattering measurement was performed by a method employing a spin polarization analysis, which allows unambiguous separation of coherent from incoherent scattering. The coherent scattering differential cross section determined in absolute units was compared with calculated curves based on the result of molecular dynamics simulation of atactic polystyrene. The simulation was performed with a united atom model and an all atom model, in both of which the bond lengths were held fixed and the phenyl group was constrained to a rigid, planar hexagon. The curves calculated from the united atom model were seen to agree fairly well with the experimental data within the experimental uncertainties due to counting statistics. The all atom model, however, gave a less satisfactory agreement—a result, which is similar to the one presented in a previous paper where X-ray scattering data in the literature were compared with simulation results. From the simulation, six different pair distribution functions giving the correlations among carbons, backbone hydrogens, and phenyl hydrogens were calculated, and from them the corresponding partial structure factors were evaluated to see the contributions which each type of pair makes to the overall neutron scattering curves.

Introduction

The nature of the short-range order present in bulk amorphous polymers has been the subject of continuing research interest by many. The question is whether there exists in amorphous polymers a local structure more ordered or more complicated than is found in simple liquids. The possible existence of a well-defined structural element such as a nodule or a meander structure, once hotly debated,[1] now appears largely discounted, but clear evidence presenting some alternative viewpoints has not been easily forthcoming. The question is nevertheless an important one since many of the mechanical and dynamic properties of polymer melts and glasses have to be explained ultimately in terms of their short- and long-range structure.

Scattering of X-rays and neutrons is by far the most effective way of probing the local structure, and yet interpretation of scattering data in terms of their structure is by no means straightforward, especially in the case of amorphous polymers. Converting the scattering intensity data to real space information by Fourier transformation is helpful but does not solve the problem, since in the resulting radial distribution function so many different pair correlations overlap to produce a few broad peaks that one can only sort them out by resorting to a molecular model. Moreover, past experiences[2-6] showed that attempts to reproduce the experimental scattering curve or radial distribution function from a model were not very successful when the model considered consisted merely of a limited number of segments, an isolated chain of random configuration, or a disordered crystalline structure. Clearly we need a model of a "bulk" amorphous polymer, in which account is taken not only of the conformational properties of a single chain but also of the intermolecular effect arising from nonbonded interactions. In recognition of this we have now undertaken to apply the molecular dynamics simulation technique to a model of bulk atactic polystyrene at its realistic density. The X-ray and neutron scattering data are then taken not as the primary source of data from which to obtain structural information directly but rather as the primary criteria to test whether the simulation was performed successfully enough. Once the model is confirmed as essentially correct, the simulation results can then be analyzed in great depth to extract the necessary structural information of the polymer.

Details of the MD simulation method and the models used were described in the previous paper[7] (hereafter called part 1). From the simulation results we then calculated X-ray scattering patterns, from which we also derived the (smeared) radial distribution function using the procedure[4,8-10] normally employed for analysis of experimental X-ray data. The MD simulation was performed on two models of atactic polystyrene, the united atom model in which the hydrogens were combined to the carbons to which they were attached and the all atom model with explicit hydrogens. The X-ray scattering curves and the radial distribution functions calculated on the basis of the united atom model results were found to agree well with experimental data in the literature, within the uncertainties of the experimental data themselves. The all atom model, surprisingly, gave results which clearly deviated from experiment in some important respect. This

† Present address: Department of Polymer Chemistry, Tokyo Institute of Technology, Meguro-ku, Tokyo, Japan.
‡ Present address: Exxon Research and Engineering Co., Annandale, NJ 08801.
§ Present address: Department of Physics, Jochiwon Campus, Korea University, Korea.
® Abstract published in *Advance ACS Abstracts*, August 15, 1994.

0024-9297/94/2227-5674$04.50/0

of course reflects some shortcomings in the force field parameters used in the model which are unknown to us at this time. As a further test for the validity of our simulation, in this work we measure neutron scattering from polystyrene samples and compare the result with curves calculated from the simulation. For this purpose, we synthesize four atactic polystyrene samples in which some of the hydrogens are replaced with deuteriums. Having four isotopic isomers of the same polymer affords an increased amount of information[5] on the structure of the polymer and consequently an enhanced opportunity for validating the simulation. A description of the short-range structure deduced from detailed analysis of the MD data will be presented in a separate, forthcoming paper.

The structural information we seek is contained in the intensity of coherently scattered neutrons. For samples containing a fair amount of hydrogen, the large incoherent scattering cross section of a hydrogen atom makes accurate evaluation of coherent scattering difficult. Although the total incoherent scattering cross section is, in principle, independent of scattering vector q and could be subtracted as a constant background from the total scattering, in practice the incoherent part turns out to depend on q[11,12] due to instrumental factors. To eliminate the uncertainty due to incoherent scattering, in this work we have adopted the technique of neutron spin polarization analysis. The utility of the technique in the study of amorphous polymers was demonstrated by Gabrys et al. with measurements on poly(methyl methacrylate).[12] The method rests on the fact[13-15] that coherent scattering occurs without change in the neutron spin, while two-thirds of the incoherent scattering is accompanied by flipping of the spin from $^1/_2$ to $-^1/_2$ or vice versa. Therefore, the coherent and incoherent scattering differential cross sections are given by

$$(d\sigma/d\Omega)_{coh} = (d\sigma/d\Omega)_{nsf} - \frac{1}{2}(d\sigma/d\Omega)_{sf} \quad (1)$$

$$(d\sigma/d\Omega)_{inc} = \frac{3}{2}(d\sigma/d\Omega)_{sf} \quad (2)$$

where $(d\sigma/d\Omega)_{sf}$ is the differential cross section of the scattering accompanied by spin flipping, and $(d\sigma/d\Omega)_{nsf}$ is the same not accompanied by spin flipping. Interposing a spin polarizer in the incident beam and monitoring the intensities of the neutrons through a spin-polarization analyzer, it is possible to measure $(d\sigma/d\Omega)_{sf}$ and $(d\sigma/d\Omega)_{nsf}$ and then to evaluate the coherent and incoherent cross sections separately by eqs 1 and 2.

Experimental Section

Materials. Four samples of polystyrene with different isotopic compositions, namely, a perdeuterated polystyrene (D8), a polystyrene with its phenyl hydrogens deuterated (D5), one with its backbone hydrogens deuterated (D3), and one with all its hydrogens unmodified (H8), were synthesized by anionic polymerization. Their M_n and M_w/M_n ratios are as follows: 60 000 and 1.08 for D8; 46 000 and 1.04 for D5; 51 000 and 1.06 for D3; and 46 000 and 1.05 for H8. The samples were molded into cylinders of 4 mm diameter and 4 cm in length. Some of these samples were rapidly cooled to room temperature from above T_g, and some were annealed at 90 °C over a month, but no differences in scattering, within the precision of our measurement, were detected between the quenched and annealed samples.

Neutron Scattering Measurement. The measurements were performed at the National Institute of Standards and Technology on BT2 and BT9 triple axis powder spectrometers, of which the former was equipped with a spin polarization analysis option. All measurements were carried out at room temperature. The incident wavelengths used were 2.35 and 1.52 Å for BT2 and BT9, respectively. The ranges of scattering wave vector q studied were 0.3–4.0 Å^{-1} for BT2 and 0.35–6.2 Å^{-1} for BT9. The transmission factors of the samples were measured to be 0.776, 0.597, 0.470, and 0.303 for D8, D5, D3, and H8 on BT2 and 0.820, 0.745, 0.671, and 0.562 on BT9, respectively. Absorption correction was applied by using the method described by Rouse and Cooper.[16] Correction for multiple scattering was applied by estimating the latter in accordance with the results obtained by Blech and Averbach[17] and by Mayers and Cywinski.[18] Scaling of the intensity data to absolute units was performed by comparing them with the scattering from a vanadium rod used as an incoherent scattering standard on BT9. Correction for the imperfect polarization efficiency of the instrument was performed as described by Williams.[19]

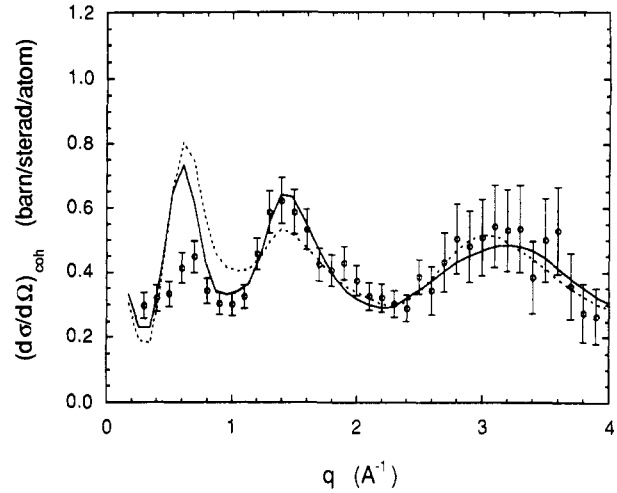

Figure 1. Coherent scattering differential cross section of perdeuterated polystyrene measured with spin polarization analysis (circles) compared with the result calculated from the united atom model (solid line) and from the all atom model (broken line).

Method of MD Simulation

The models and methods used for the MD simulation have been described in detail in part 1. Some salient points are repeated here. The basic MD cubic cell of edge length 2.38 nm contains an atactic polystyrene chain consisting of 80 monomer units and its images created by the periodic boundary conditions; the resulting bulk density is equal to 1.028 g/cm^3. In the united atom model, the hydrogen atoms are absorbed into the carbon atoms to which they are attached, but in the all atom model the hydrogens are explicitly represented. In both models, the bond lengths are kept fixed by means of the SHAKE algorithm[20] and the phenyl group is maintained as a rigid hexagonal structure by means of the constrained geometry algorithm of Ciccotti et al.[21] All the force field parameters used are listed in part 1. MD runs were made under constant volume and temperature, starting from three different initial configurations. In configurations A and B the chain has the same stereochemical sequence of monomers, generated by a Bernoulli run designed to produce 40% meso diads. Configuration B was derived from configuration A by running the MD program through intermediate states of very low density and high temperature, to produce a state of chain packing in the MD cell that is very different in configuration B than configuration A. In configuration C the chain has an entirely different stereochemical sequence of monomers generated by an independent Bernoulli run.

Results and Discussion

The coherent scattering cross sections $(d\sigma/d\Omega)_{coh}$, evaluated by means of the spin polarization analysis as described above, are given in Figures 1–4 for the four

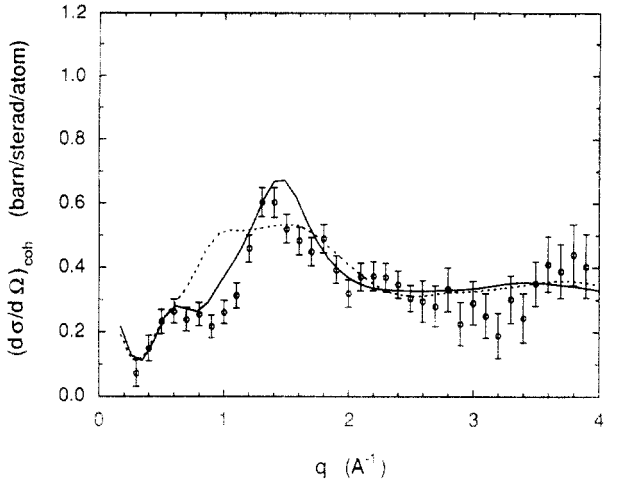

Figure 2. Similar to Figure 1, but for polystyrene with its phenyl groups deuterated.

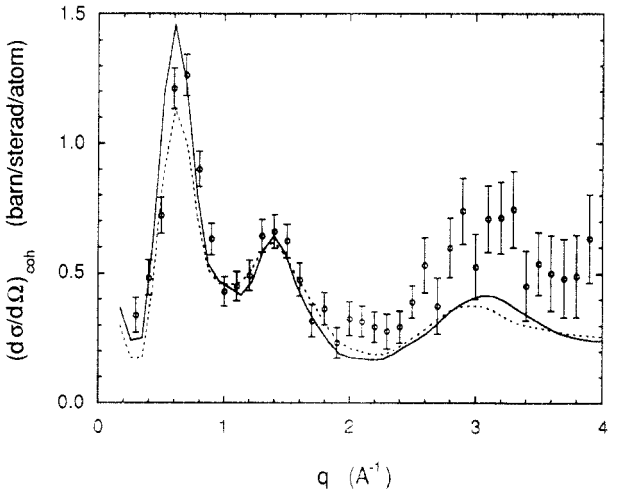

Figure 3. Similar to Figure 1, but for polystyrene with its aliphatic backbone hydrogens replaced by deuteriums.

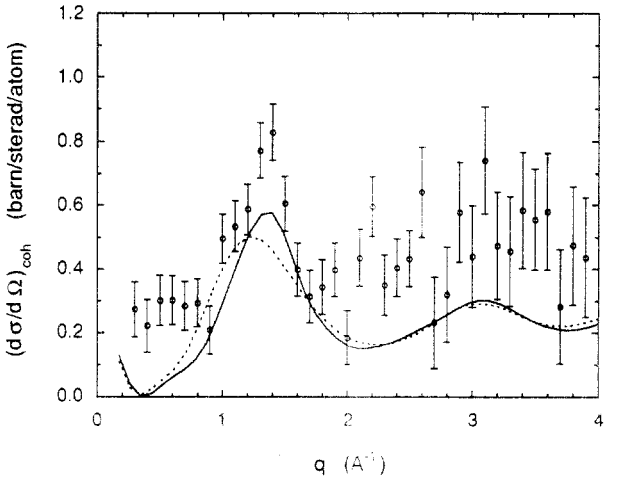

Figure 4. Similar to Figure 1, but for hydrogenous polystyrene.

selectively deuterated polystyrene samples. The ordinate scale is in absolute units (barns/steradian) per atom. The error bars which are fairly large reflect the difficulty of accumulating large enough numbers of counts when a polarization analysis is superimposed. The error bars are particularly large in the case of the hydrogenated sample H8 in Figure 4 because of the large incoherent scattering cross section of hydrogen atoms. After our measurements were substantially completed, it was learned that Schärpf et al.[6] employed four polystyrene samples of very similar isotopic compositions as ours and determined the coherent scattering differential cross section. Their results substantially agree with ours, within experimental error, except that the scattering curve obtained with their perdeuterated sample is very similar to ours in shape but the intensity level is about half of ours throughout the whole q range.

The solid lines in Figures 1–4 are those calculated from the MD simulation with the united atom model, and the broken lines are those calculated from the all atom model. For the purpose of these calculations, the united atom model MD program was run for 500 ps each starting from configurations A, B, and C, and the atomic coordinates were recorded at intervals of 1 ps. Before the neutron scattering intensity was calculated according to the method described below, the hydrogens (or deuterium atoms) were placed in the appropriate positions relative to the carbon atoms. The intensities were calculated for each of the 500 sets of atomic coordinates and their average was evaluated for each of the runs. These three averaged intensity curves showed only minor differences among them (see part 1). The three curves were further combined into a single curve which is then plotted in Figures 1–4. Next, the atomic configurations obtained at the end of the three 500 ps runs were taken as the starting configurations for the all atom model. The MD program was run for 200 ps with each configuration, and the atomic trajectories were again recorded at intervals of 1 ps. The intensities calculated from the 200 coordinate sets with each run were again combined all together before they were plotted as broken lines in Figures 1–4.

The agreement between the experiment and the calculated results is fairly satisfactory. In all cases the positions of the peaks and the overall shape of the curves are well reproduced, although some discrepancies in the peak heights are apparent. In part 1 it was shown that the calculated X-ray scattering curve agreed much better with experiment if the united atom model was used instead of the all atom model. The same is true in the present case also, and this is especially evident with the phenyl deuterated sample in Figure 2, where the slight dip in the intensity around $q = 0.9$ Å^{-1} shown in experiment is well reproduced by the united atom calculation but is missed completely by the all atom calculation. A better agreement with the united atom model compared to the all atom model can also be noted with the perdeuterated sample in Figure 1, especially with regard to the height of the second peak at around $q = 1.4$ Å^{-1}. In the case of the hydrogenous sample, shown in Figure 4, the shape of the curve agree well between the experiment and calculation but the overall levels of the two do not match. This suggests that the process of data correction applied to experimental results, either to subtract the incoherent scattering or to place the measured intensity on an absolute scale, might not have been performed accurately enough for the hydrogenated sample which has a particularly large incoherent scattering cross section. In part 1 we have concluded that the X-ray intensity curve calculated from our united atom model agrees well with experimental results, and any discrepancy between calculation and experiment is in fact comparable to the discrepancies between any two published experimental X-ray intensity curves. The same can probably be said here, and it suggests that any further refinement of our MD model has to wait until more precise neutron data become available.

For isotropic materials, the neutron coherent scattering differential cross section can be calculated according to

$$(d\sigma/d\Omega)_{coh} = \frac{1}{N}\sum_m\sum_n b_m b_n \frac{\sin qr_{mn}}{qr_{mn}} \quad (3)$$

where N is the total number of atoms in the system, b_m is the neutron scattering length of atom m, r_{mn} is the distance between atoms m and n, and the summations run over all the atoms in the system, including the term $m = n$. The differential cross section is given in units of barn/steradian per atom. In our four polystyrene samples with different isotopic substitutions, we recognize three distinct types of atomic species, carbons, hydrogens (or deuteriums) in the chain backbone (designated by symbol "b"), and hydrogens (or deuteriums) in the phenyl group (designated by symbol "p"). The structure, for the purpose of neutron scattering intensity calculation, is uniquely defined in terms of six pair distribution functions $g_{cc}(r)$, $g_{cb}(r)$, $g_{cp}(r)$, $g_{bb}(r)$, $g_{pp}(r)$, and $g_{bp}(r)$. The pair distribution function $g_{ij}(r)$ is given by

$$g_{ij}(r) = \rho_{ij}(r)/\langle\rho_j\rangle \quad (4)$$

where $\rho_{ij}(r)$ is the density of atom type j at a distance r from an atom of type i, and $\langle\rho_j\rangle$ is the average density of atom type j. Associated with each pair distribution function $g_{ij}(r)$, we can define[22] a partial structure factor $S_{ij}(q)$ by

$$S_{ij}(q) = \delta_{ij} + \langle\rho_j\rangle\int 4\pi r^2[g_{ij}(r) - 1]\frac{\sin qr}{qr}\,dr \quad (5)$$

where $S_{ij}(q)$ expresses the interference effect that arises between an atom of type i and all the atoms of type j in the system. In terms of these partial structure factors, the coherent differential cross section can be given as

$$(d\sigma/d\Omega)_{coh} = \sum_i x_i \sum_j b_i b_j S_{ij}(q) \quad (6)$$

where x_i is the atomic fraction of the type i atom, and the indices i and j both run for c, b, and p (so that terms involving both $S_{cb}(q)$ and $S_{bc}(q)$, for example, are included in eq 6). The six $S_{ij}(q)$s are common to all the four samples, and only the b_is vary from sample to sample. If there were six samples that differed in isotopic contents, then measurements of the six $(d\sigma/d\Omega)_{coh}$ would have allowed the determination of the six $S_{ij}(q)$s by solving the six simultaneous linear equations given by eq 6. Such a procedure was in fact employed with neutron scattering measurements of a liquid Cu–Sn alloy,[23] and the three partial structure factors involved were thereby determined. In the case of chloroform $CHCl_3$,[24] neutron scattering measurements on four isotopic isomers of the liquid and on a mixture of $CHCl_3$ and $CDCl_3$ were combined with X-ray scattering measurements to give all the six partial structure factors. In the present case we do not have a sufficient number of isotopically different samples to allow determination of the partial structure factors $S_{ij}(q)$ from experiment and instead will evaluate them from the MD results and examine them as an aid to understanding the short-range structure.

Parts a–f of Figures 5 give the six pair distribution functions $g_{ij}(r)$ evaluated from the MD results. The solid curves are those based on the united atom model and the broken curves on the all atom model. In our simulations the bond lengths were all kept fixed, whereas in reality the bond lengths fluctuate around their equilibrium lengths. To compensate for the stretching vibration of the bonds around their equilibrium lengths, the pair distribution functions evaluated from the simulation were convoluted with a Gaussian function with σ equal to 0.04 Å. The partial structure factors $S_{ij}(q)$ evaluated from the corresponding $g_{ij}(r)$ according to eq 5 are given in parts a–f of Figure 6. The $S_{ij}(q)$s were evaluated at q equal to integral multiples of $\pi/2r_{max}$ (where the upper integration limit r_{max} is equal to 18 Å) to minimize the spurious oscillations that arise from truncation error, as suggested by Lovell, Mitchell, and Windle.[27] Summation of these $S_{ij}(q)$s, with the values of the scattering lengths b_is appropriate to each sample, then gives the coherent differential cross sections shown in Figures 1–4.

In all the figures presented, results obtained from the all atom model as well as the united atom model are shown, since, although the former is clearly inferior, a comparison between the two models provides a useful insight into the structural details that are responsible for some of the features in the scattering curves. $S_{cc}(q)$ given in Figure 6a shows a close similarity to the experimentally determined X-ray scattering curve. This is not unexpected, since X-ray scattering arises predominantly from carbon–carbon correlations. The united atom model result clearly shows the "polymerization peak" at q around 0.7 $Å^{-1}$, whereas the all atom model, as pointed out in part 1, fails to reproduce it. If we look at the corresponding pair distribution function $g_{cc}(r)$ in Figure 5a, the most important difference that can be noted is the presence, in the united atom model, of a distinct periodic oscillation in the C–C pair correlation, with a period of about 4.5 Å, beyond r = 5 Å. Such a periodicity apparently arises from the dispositions of phenyl groups, as can be inferred on the basis of other pieces of evidence noted below. Both $S_{bb}(q)$ in Figure 6b and $g_{bb}(r)$ in Figure 5b show very little difference between the united and all atom models, suggesting that the disposition of the chain backbone (and the positions of backbone carbons and hydrogens) is essentially the same in both models and presumably is reproduced correctly. The correlation between phenyl hydrogens, as revealed by $S_{pp}(q)$ in Figure 6c, is seen to differ between the two models at small q, especially in the height of the peak at the position corresponding to the "polymerization peak". (It is, however, surprising to see that the corresponding $g_{pp}(r)$ in Figure 5c shows only minor differences between the two models spread throughout the range of r examined.) The fact that the main difference between the two models resides in the disposition of phenyl groups can be seen also from the fact that $S_{cp}(q)$ and $S_{bp}(q)$ show clear differences between the two models, whereas in $S_{cb}(q)$ the differences are smaller.

In comparing $S_{ij}(q)$ in parts a–f of Figure 6 with the corresponding $g_{ij}(r)$ in parts a–f of Figure 5, we are struck by the difficulty with which any of the peaks in $S_{ij}(q)$ can be identified with any specific structural features in the corresponding $g_{ij}(r)$. For example, all six $S_{ij}(q)$s display peaks at around 0.6 $Å^{-1}$ (negative peaks in the case of S_{cp} and S_{bp}), and yet it is difficult to discern any commonality among the six $g_{ij}(r)$s at $r \sim 10$ Å (=$2\pi/0.6$), or at any r for that matter, that might be thought of as causing the 0.6 $Å^{-1}$ peak. It has been a common practice, in looking at X-ray or neutron scattering patterns, to try to identify or associate a peak in the reciprocal space with a distinct structural feature in the real space. The results given here show that this cannot be done. Even for the main "amorphous" peak at around 1.4 $Å^{-1}$ in $S_{cc}(q)$ one has a difficulty in finding its counterpart in $g_{cc}(r)$ at $r = 2\pi/1.4 = \sim 4.5$ Å (aside from the oscillation with a period of 4.5 Å mentioned above). This shows that the Fourier transform represented by eq 5 is a very subtle process that

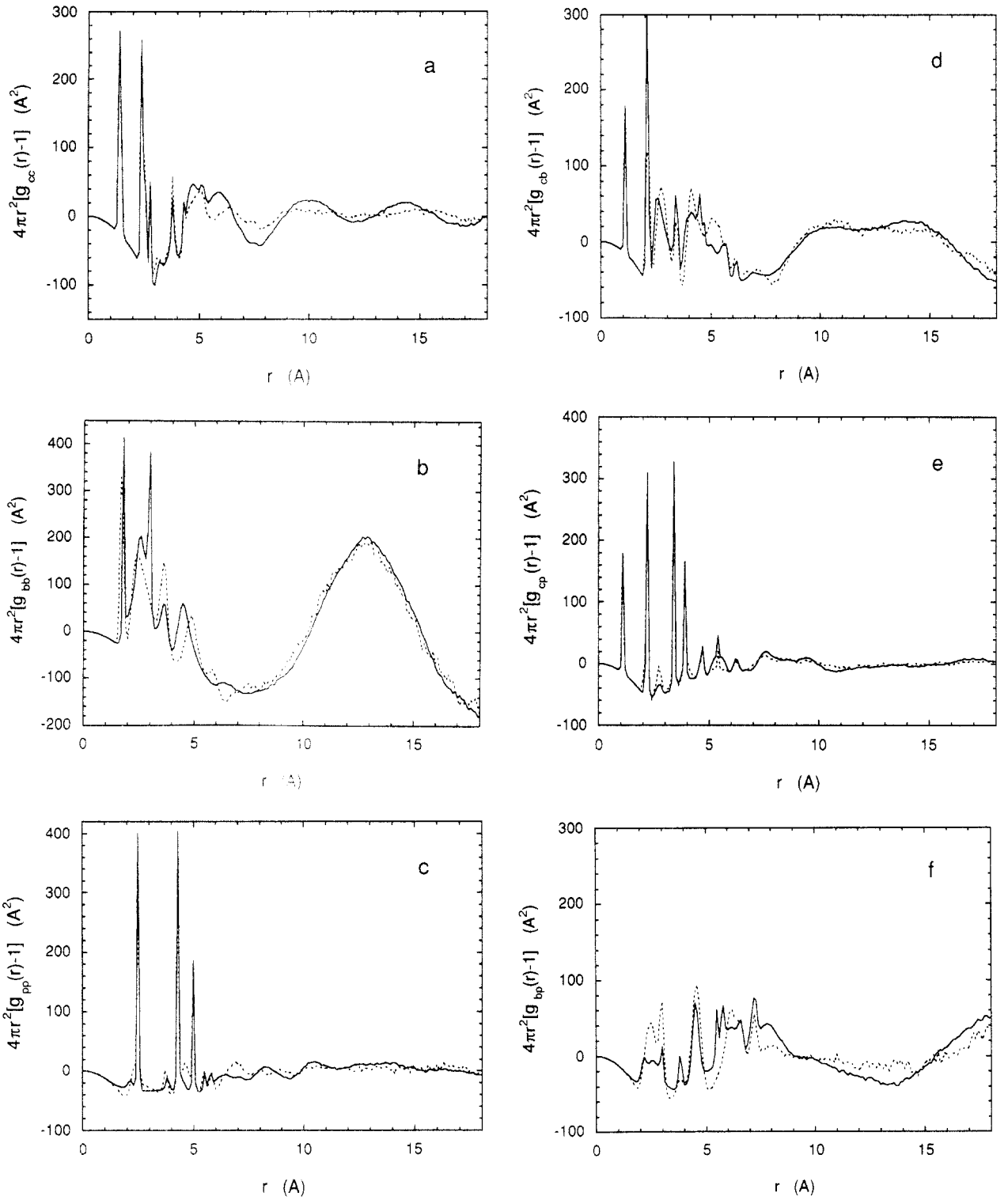

Figure 5. Pair distribution functions calculated from the united atom model (solid line) and from the all atom model (broken line). (a) Pair distribution function $g_{cc}(r)$ for carbon–carbon pairs; (b) pair distribution function $g_{bb}(r)$ for b–b pairs where *b* is a hydrogen (or deuterium) in the aliphatic backbone; (c) pair distribution function $g_{pp}(r)$ for p–p pairs where p denotes a hydrogen (or deuterium) in the phenyl group; (d) $g_{cb}(r)$; (e) $g_{cp}(r)$; (f) $g_{bp}(r)$.

cannot be easily grasped intuitively when the underlying functions $g_{ij}(r)$ and $S_{ij}(q)$ are as complicated as in polymers in which both intramolecular and intermolecular correlations are involved. Unlike crystalline materials with which at least the lattice parameters can always be derived directly from the scattering curve, it is more difficult in the case of polymer liquids and glasses to obtain real space information by a direct analysis of the diffraction data. As mentioned earlier, when a sufficient number of samples with different isotopic substitutions are available, measurements of neutron scattering data with each of these samples will eventually enable the determination of partial structure factors of all the different atomic pairs in the sample. A knowledge of the partial structure factors by themselves, however, does not necessarily make it easier to obtain clues to real space structure either, as the discussion above suggests. It appears that the only really fruitful approach would be to perform molecular modeling (by any of the methods such as MD, Monte Carlo, or molecular mechanics) of a realistic bulk system and deduce the structural information from the simulation results, using the experimental scattering curves mainly as a means

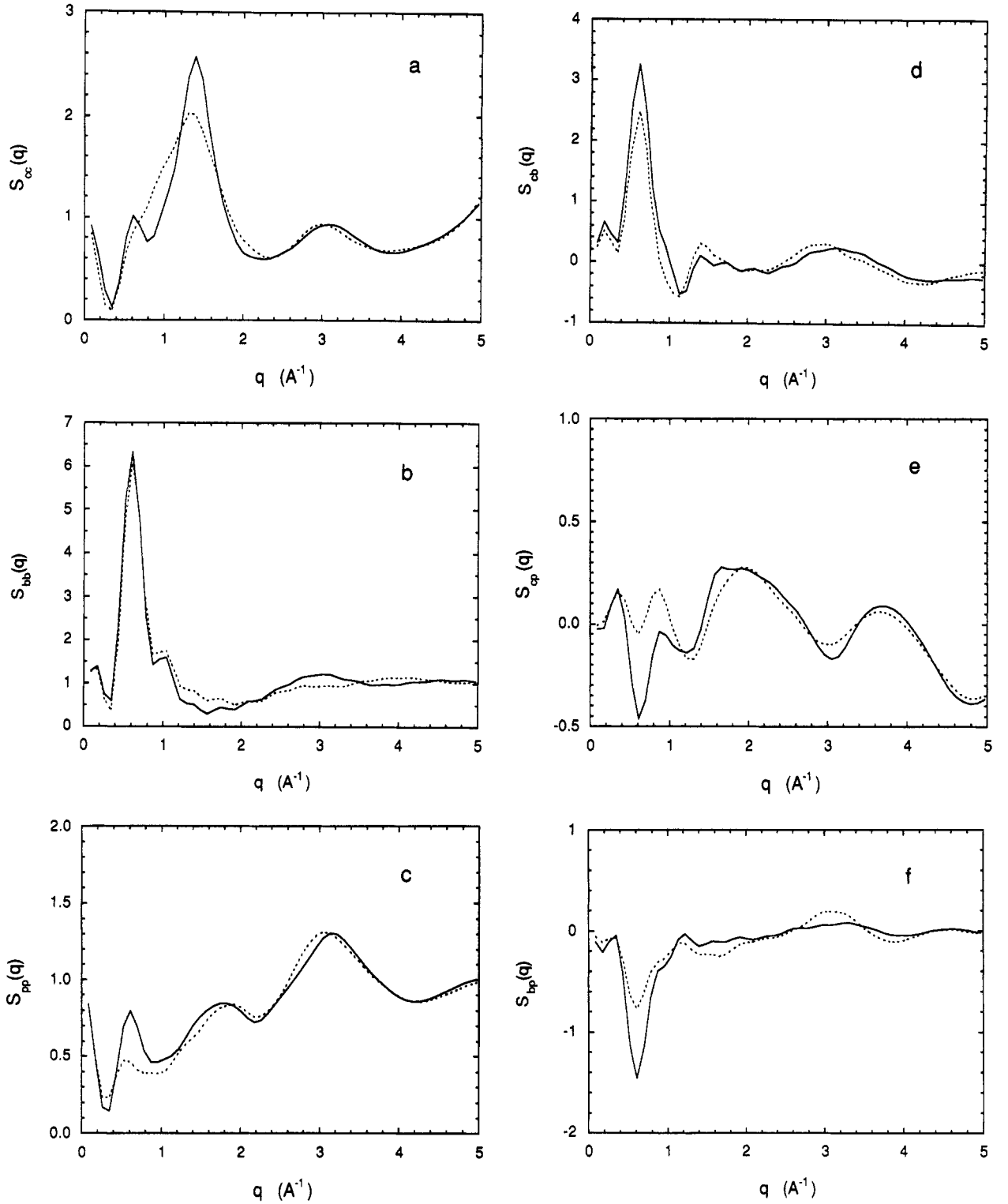

Figure 6. Partial structure factors calculated, according to eq 5, from the united atom model (solid line) and from the alll atom model (broken line). (a) $S_{cc}(q)$; (b) $S_{bb}(q)$; (c) $S_{pp}(q)$; (d) $S_{cb}(q)$; (e) $S_{cp}(q)$; (f) $S_{bp}(q)$.

of ensuring that the model is realistic. When reliable experimental data are available, one may "refine" the parameters defining the model by systematically adjusting them to achieve successively better agreement with experiment, in a way analogous to the process of successive refinement employed in the crystal structure determination from X-ray diffraction data. The amount of information that is contained in the scattering curve of an isotropic amorphous material is very limited in comparison to that available in a diffraction pattern of a crystalline material, and therefore the enhancement of information achieved by means of isotropic substitution should be a very valuable help.

Summary

Four isotopic isomers of atactic polystyrene, namely, a perdeuterated polystyrene, a polystyrene with its phenyl groups deuterated, one with its aliphatic hydrogens deuterated, and a hydrogenous polystyrene, were synthesized by anionic polymerization. Neutron scattering from these samples was measured, for the q range between 0.3 and 4 Å^{-1}, with BT2 and BT9 powder spectrometers in NIST of which the former was equipped with a neutron spin polarization analysis option. By separately measuring the intensities of scattering that occur with and without spin flip, it was possible to separate the coherent scattering

unambiguously from the incoherent scattering.

Molecular dynamics simulation of bulk atactic polystyrene was performed, as described in the previous paper, using a united atom model and an all atom model, in both of which bond lengths were held fixed and the phenyl group was constrained to a rigid, planar hexagon. The basic MD cell contained an atactic chain consisting of 80 styrene monomer units and the chains created by the periodic boundary conditions, packed to a density of 1.028 g/cm^3. The programs were run from three different chain configurations: two with a polystyrene molecule having the same stereochemical sequence of monomers but after very different thermal histories and the third with a molecule having an entirely different sequence. The neutron coherent scattering differential cross sections were calculated by taking averages over the trajectories obtained from these three configurations.

The curves calculated from the simulation agree fairly well with the experimental results with regard to both the absolute intensity and the positions and shapes of the peaks for all four isotopic samples of polystyrene. With the united atom model, the discrepancies were, in general, not more than the uncertainties in the data due to counting statistics. The agreement with the all atom model was clearly inferior. In part 1 it was similarly shown that the X-ray scattering intensity curve calculated from the united atom model agreed well with experimental data in the literature, but the all atom model gave an X-ray scattering curve which failed to reproduce the "polymerization" ring. In comparing the pair distribution functions and the partial structure factors calculated from the united atom model with those from the all atom model, it appears that the fault with the latter model appears to reside in its inability to reproduce the phenyl–phenyl correlations properly, due to some unknown shortcomings of the force field parameters used.

The pair distribution functions derived from the simulation and the partial structure factors obtained from them by Fourier transformation show the difficulty of interpreting either of them in terms of clearly identifiable structural features. This is because with polymers intramolecular and intermolecular correlations overlap severely making the pair distributions too complex, even when clear distinctions are made, for example, between hydrogens in the backbone and those in the phenyls. Instead of attempting to interpret the scattering curves or their Fourier transforms directly, the more fruitful approach should be to take the scattering data mainly as the means of testing the validity of a molecular modeling and then to deduce the structure solely by analyzing the simulation results.

Acknowledgment. This work was supported in part by NSF Grant DMR8909232. The computation performed in this work was carried out on the Cray Y-MP/864 at the Ohio Supercomputer Center, and the generous allocation of cpu time is greatly appreciated.

References and Notes

(1) See papers in: *Faraday Discuss. Chem. Soc.* **1979**, *68*.
(2) Mitchell, G. R.; Windle, A. H. *Polymer* **1984**, *25*, 906.
(3) Adams, R.; Balyuzi, H. H. M.; Burge, R. E. *J. Mater. Sci.* **1978**, *13*, 391.
(4) Wignall, G. D.; Longman, G. W. *J. Mater. Sci.* **1973**, *8*, 1439.
(5) Cervinka, L.; Fischer, E. W.; Hahn, K.; Jiang, B.-Z.; Hellmann, G. P.; Kuhn, K.-J. *Polymer* **1987**, *28*, 1287.
(6) Schärpf, O.; Gabrys, B.; Peiffer, D. G. ILL Report No. 90SC26T, Grenoble, France, 1990.
(7) Mondello, M.; Yang, H.-J.; Furuya, H.; Roe, R. J. *Macromolecules* **1994**, *27*, 3566.
(8) Wecker, S. M.; Davidson, T.; Cohen, J. B. *J. Mater. Sci.* **1973**, *7*, 1249.
(9) Schubach, H. R.; Nagy, E.; Heise, B. *Colloid Polym. Sci.* **1982**, *259*, 789.
(10) Warren, B. E. *X-ray Diffraction*; Addison-Wesley: Reading, MA, 1969.
(11) Maconnachie, A. *Polymer* **1984**, *25*, 1068.
(12) Gabrys, B.; Higgins, J. S.; Schärpf, O. *J. Chem. Soc., Faraday Trans. 1* **1986**, *82*, 1923.
(13) Williams, W. G. *Polarized Neutrons*; Clarendon Press: Oxford, England, 1988.
(14) Moon, R. N.; Riste, T.; Koehler, W. C. *Phys. Rev.* **1969**, *181*, 920.
(15) Schärpf, O. *Neutron Scattering in the Nineties*; International Atomic Energy Agency: Vienna, 1985; p 85.
(16) Rouse, K. D.; Cooper, M. J. *Acta Crystallogr.* **1970**, *A26*, 682.
(17) Blech, I. A.; Averbach, B. L. *Phys. Rev.* **1965**, *137*, A1113.
(18) Mayers, J.; Cywinski, R. *Nucl. Instrum. Method Phys. Res.* **1985**, *A241*, 519.
(19) Reference 13, p 221.
(20) Ryckaert, J. P.; Ciccotti, G.; Berendsen, J. J. C. *J. Comput. Phys.* **1977**, *23*, 327.
(21) Ciccotti, G.; Ferrario, M.; Ryckaert, J.-P. *Mol. Phys.* **1982**, *47*, 1253.
(22) Note that the definition of the partial structure factor given in eq 5 is slightly different from those given by others; cf. refs 23–26.
(23) Enderby, J. E.; North, D. M.; Egelstaff, P. A. *Philos. Mag.* **1966**, *14*, 961.
(24) Bertagnolli, H.; Chieux, P. *Mol. Phys.* **1984**, *51*, 617.
(25) Enderby, J. E. In *Physics of Simple Liquid*; Temperley, H. N. V., Rowlinson, J. S., Rushbrooke, G. S., Eds.; North-Holland: Amsterdam, The Netherlands, 1968; Chapter 14, p 611.
(26) Hansen, J.-P.; McDonald, I. R. *Theory of Simple Liquids*, 2nd ed.; Academic Press: New York, 1986; p 103.
(27) Lovell, R.; Mitchell, G. R.; Windle, A. H. *Acta Crystallogr.* **1979**, *A35*, 598.